Advanced path tracking control for off-road mobile robots

Roland Lenain*, Benoit Thuilot†, Christophe Cariou*, Philippe Martinet†
* Cemagref
24, av. des Landais
63172 Aubière Cedex France
roland.lenain@cemagref.fr
† LASMEA
24, av. des Landais
63177 Aubière Cedex France
benoit.thuilot@lasmea.univ-bpclermont.fr

***Abstract*— The growing social needs in terms of environmental and efficiency issues make the development of automated mobile robots in an off-road context more and more important. Nevertheless, the accurate control of such robots in natural environment requires to take into account several uncertain phenomena, in particular to the varying grip conditions and various delays. If complex models are available to address such problems, their numerous parameters appearing to be variable in an off-road context make them hardly tractable to design an efficient control law.**

In this paper, an adaptive and predictive control algorithm, based on an extended kinematic model and dedicated to four wheeled steered mobile robots in off-road conditions is proposed for high accurate path tracking applications. The effects of variable low grip conditions are accounted in a kinematic representation thanks to additional variables updated by an observer. This allows the derivation of an adaptive backstepping control approach, able to preserve the accuracy of the path tracking despite of low grip conditions. In addition, a predictive curvature control allows to compensate for the large delays originated from the actuators used on off-road heavy vehicles. The relevance of theoretical developments detailed in this paper are investigated through full scale experiments on both an agricultural tractor (two steering wheels) and a Robucar TT mobile robot (four steering wheels).

I. INTRODUCTION

The potential benefits of off-road mobile robot applications in various fields (such as exploration, public security, farming or surveillance) show the importance of designing relevant autonomous vehicle control strategy. In particular, the various situations encountered in natural terrains, as well as the complexity and the uncertainty of the interaction between robots and their environment require the use of advanced control techniques.

Numerous control strategies have been investigated in the literature. Nevertheless, such classical control laws rely on a model based on too restrictive assumptions when off-road environment is considered. In particular, the Ackermann model (or bicycle model) assuming rolling without sliding (RWS) is often used, as it offers interesting properties from control point of view. It can indeed be turned easily into an exact linear form using for example flatness feedback control law (see [7]) or chained system theory (see [16]). These techniques, particularly suitable for path tracking problems, are unfortunately not relevant when sliding occurs. Their performances are indeed strongly depreciated in such cases (see for instance [14]). To address such problems, some robust approaches can be proposed without requiring explicit modeling of encountered phenomena (for instance [3] or [20]). Such a point of view is nevertheless restrictive, since it does not consider the potential knowledge of the perturbation dynamics.

Another approach allowing to address the different phenomena occurring in natural environment - and more particularly the wheel slippage - lies in the use of dynamical models (such as in [15]). Such representations indeed permit to describe the influence of contact forces on mobile robot behavior. However, contact models (such as [1], [4] or [17] for models survey) require the introduction of numerous parameters, depending on ground conditions, load repartition, and then subject to large on-line variations in an off-road context. Moreover, the estimation of such parameters is hardly feasible on-line with standard perception systems (as can be seen in [5] or in [8]). As a consequence, control laws derived from such models cannot be used with high efficiency in practical application.

In order to avoid the use of complete tire/soil contact models, while still relying on a model-based approach, this paper proposes alternative descriptions of mobile robot motion. These representations, taking part of both kinematic and dynamic views (in a comparable way as in [9] or in [19]), are called extended kinematic models. They indeed rely on an Ackermann description, but take part of dynamic modeling to introduce a limited number of parameters, observable on-line. Consequently, these models are representative of the vehicle motion in presence of sliding. This approach, previously designed for car-like vehicles is here extended for two-steered axles mobile robots. The modeling as well as the sliding estimation required, are presented in the first part of this paper. In a second part, the motion control of such robots is investigated through different techniques, demonstrating the potentialities of such models. An observer based adaptive control, coupled with predictive curvature servoing, is then detailed. Finally, the performances of the proposed control strategy for accurate path tracking are demonstrated experimentally in the last section.

II. MOBILE ROBOT MODELING

A. Classical kinematic point of view

As the approach proposed in this paper consists in preserving a simple model structure, we preliminary consider the celebrated Ackermann model under rolling without sliding assumption at the wheel/ground contact. As depicted on

the figure 1, this model describes the generic four wheeled steered vehicle to be controlled as a bicycle model.

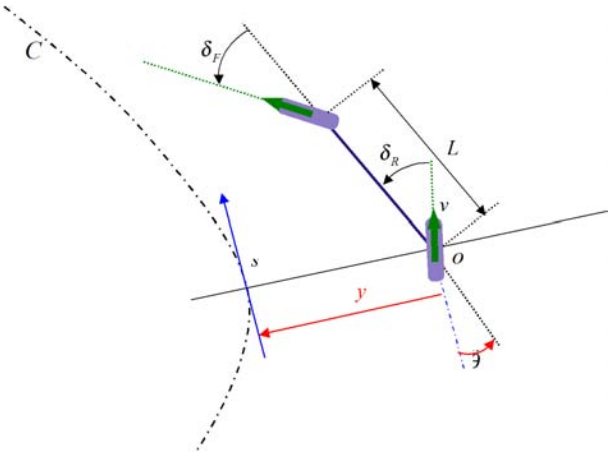

Fig. 1. Classical kinematic model parameters

In the framework of path tracking applications, the description of vehicle motion is described with respect to the desired path - preliminary computed or recorded. Using this point of view, the notations used in the sequel are shown in figure 1 and listed below:

- $\mathcal{C}$ is the path to be followed,
- O is the center of vehicle virtual rear wheel. This point is assumed to be the control point,
- s is the curvilinear coordinate of the closest point belonging to $\mathcal{C}$. $c(s)$ denotes the curvature of $\mathcal{C}$ at that point.
- y and $\tilde{\theta}$ are respectively lateral and angular deviation of the vehicle with respect to reference path $\mathcal{C}$ (see Figure 1).
- δ_F and δ_R are respectively the virtual front and rear wheel steering angles. They are the input variables.
- v is the vehicle linear velocity, considered here as a parameter. Its value may be time-varying during the vehicle evolution but the control of this variable is not addressed in this paper.
- L is the vehicle wheelbase.

Using these notations, the equations of mobile robot motion with respect to the desired path can be derived. In a state space representation, $x = [\ s \quad y \quad \tilde{\theta}\ ]^T$ denotes the state vector, while $\delta = [\ \delta_F \quad \delta_R\ ]^T$ is the input vector. Considering that the two virtual wheels (front and rear) obey rolling without sliding conditions, the kinematic evolution of these mobile robots can be described by the classical system (1) (see [16] for more details).

$$\dot{x} \quad = \quad f(x, \delta) \tag{1}$$

with

$$f = v \begin{bmatrix} \frac{\cos(\tilde{\theta}+\delta_R)}{1-c(s)y} \\ \sin(\tilde{\theta}+\delta_R) \\ \cos\delta_R \frac{\tan\delta_F - \tan\delta_R}{L} - \frac{c(s)\cos(\tilde{\theta}+\delta_R)}{1-c(s)\,y} \end{bmatrix} \tag{2}$$

The function f exists under the assumption $y \neq \frac{1}{c(s)}$. This is ensured in practice since, on one hand, actual reachable path curvatures are quite small, and on the other hand, when properly initialized, the vehicle remains close to $\mathcal{C}$. The lateral deviation is thereby always smaller than the radius of curvature of $\mathcal{C}$. As a result, the non-restrictive assumption (3) can be made and will be used in the sequel.

$$|y| < \frac{1}{|c(s)|} \quad \Rightarrow \quad 1 - c(s)\,y > 0 \tag{3}$$

B. Extension to sliding influence

As pointed out previously, such a model is not complete enough to be representative of mobile robot motion when adherence conditions do not meet the rolling without sliding assumption. If dynamic models can be exploited to account for wheel slippage influence, they require an important number of variables and parameters, which are difficult to estimate in off-road context. Alternatively, the kinematic model (1) is here extended in order to account for bad adherence properties. As sliding modifies the mobile robot behavior, and more particularity violates the non holonomic constraints, some additive parameters or variables must be introduced. In the frame of path tracking, sliding interacts with the two state variables (y and $\tilde{\theta}$) expected to be controlled. As a consequence, at least two variables (or parameters) must be introduced to reflect such a phenomenon. Several possibilities for sliding introduction can be considered:

1) Behavior Based Kinematic Model - BBKM: In this point of view, the effects of sliding on mobile robot motion are accounting without considering any contact model. Preliminary experiments carried out with a control law designed under rolling without sliding assumption reveal that the non-holonomy is violated by both a rotational and translational motion. Extending the approach proposed in [11], sliding influence can be accounted by the addition of two sliding parameters, gathered in the vector $\xi = [\ 0 \quad \dot{Y}_P \quad \dot{\Theta}_P\ ]^T$. It impacts the model (1) as following:

$$\dot{x} \quad = \quad f(x, \delta) + \xi \tag{4}$$

This perturbation vector ξ then allows to reflect the additional motions caused by the bad adherence properties and, if relevantly identified, to describe accurately mobile robot evolution when sliding occurs.

2) Tire Based Kinematic Model - TBKM: As said previously, in a dynamic representation of mobile robot motion, the contact forces are derived thanks to a tire model. In most of such models, lateral forces rely on side slip angle variables, representative of the difference between tire orientation and actual velocity vector direction. This notion of side slip angles can be introduced in the Ackermann model: let us consider a bicycle model with two side slip angles denoted by vector $\beta = [\ \beta_F \quad \beta_R\ ]^T$ for the front and rear wheel. Relying on the actual speed vector directions, a new model (5) can be derived from (1) (such as in [12]).

$$\dot{x} \quad = \quad f(x, \delta - \beta) \tag{5}$$

As previously, the two additional parameters reflect the impact of sliding. Nevertheless, in this point of view, the nonholonomic structure of motion equations is preserved: sliding parameters indeed appear in trigonometric functions in the model (5) and consequently act as non linearity. As a result, compared to model (4), the effect of sliding is limited (bounded by trigonometric functions).

C. Additive variables estimation

If these two alternative kinematic models are theoretically able to be representative of mobile robot motions in presence of sliding effects, a key point is the relevant knowledge of the value of additional parameters. In both of parameters sets, a direct measurement via dedicated sensors is hardly feasible. As a result, $(\dot{Y}_P, \dot{\Theta}_P)$ as well as (β_F,β_R) must be reconstructed through the available measurements. In practice, the variables assumed to be known are the position and the orientation of the robot. In a path tracking frame, this means that y (lateral deviation) and $\tilde{\theta}$ (angular deviation) are known.

A first solution for indirect estimation could consist in including sliding parameters in the state vector without explicit evolution model. This leads to an observable system (as shown in [13]): there is indeed two unknowns in extended models while at least two state variables (three when considering s) are measured. Nevertheless, the observation matrices are generally bad conditioned, leading to unsuitable results.

In this paper, the sliding parameters are alternatively considered as input variables of extended models. As depicted on the figure 2, an observation loop acting in parallel to classical control loop is defined. The objective of this second loop is to control sliding parameters in order to ensure the convergence of model outputs to the measured state variables.

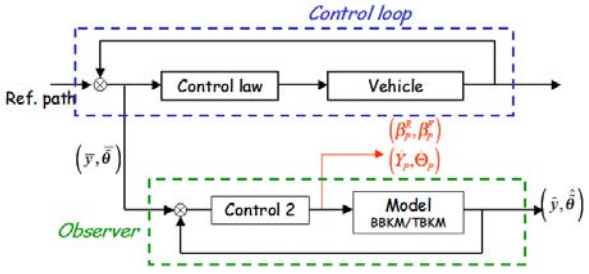

Fig. 2. Observer principle scheme

More precisely, let us denote by $X = [\ y \quad \tilde{\theta}\ ]^T$ the state vector dedicated to observation. The observed state $\hat{X}$ relies on sliding parameters. A control law is then expected to be designed for these sliding parameters in order to ensure the convergence of $\hat{X}$ to the measured state $\bar{X}$. Such a convergence will ensure that the siding parameters are representative of the actual robot behavior.

Let us denote the observed error by e:

$$e = \hat{X} - \bar{X} \tag{6}$$

This error is expected to be brought to zero by imposing an exponential convergence such as:

$$\dot{e} = G \cdot e \tag{7}$$

with G a chosen Hurwiz matrix tuning observer performances.

According to model (4) defining the evolution of BBKM (Behavior Based Kinematic Model), the desired error dynamics (7) can be reached thanks to the following law, which constitutes the estimation of the first parameters set:

$$\hat{\xi} = G \cdot e - f^{Obs}(\hat{X}, \delta) + \dot{\bar{X}} \tag{8}$$

where $\dot{\bar{X}}$ is the filtered numerical derivative of the measured state vector and f^{Obs} iconsists of the two last lines of function f defined in (2).

As mentioned before, in the TBKM (Tire Based Kinematic Model) sliding parameters appears as non linearities. The observation equation ensuring the error dynamics (7) is then less trivial. It can nevertheless be designed by linearizing model (5) around null sideslip angles (as their value does not exceed some degrees in practice). These calculations, following the same formalism as in [13], leads to the following observer equation:

$$\hat{\beta} = B(\hat{X}, \delta)^{-1} \left\{ G \cdot e - f^{Obs}(\hat{X}, \delta) + \dot{\bar{X}} \right\} \tag{9}$$

where $B(\hat{X}, \delta) = \frac{\partial f^{Obs}(X, \delta - \beta)}{\partial \beta}$ defined as the partial derivative of the two last lines of model (5) with respect to side slip angles and evaluated at $(\beta_F, \beta_R) = (0, 0)$. B can be written as:

$$B(\hat{X}, \delta) = v \begin{bmatrix} 0 & \cos(\hat{\tilde{\theta}} + \delta_R) \\ \frac{\cos \delta_R}{L \cos^2 \delta_F} & \frac{c(s) \sin(\hat{\tilde{\theta}} + \delta_R)}{1 - c(s)\hat{y}} - \frac{1}{L \cos \delta_R} \\ & -\sin \delta_R \frac{\tan \delta_F - \tan \delta_R}{L} \end{bmatrix} \tag{10}$$

and is invertible in path tracking application ($v \neq 0$).

D. Extended model validation

In order to validate the capabilities of the extended models to describe accurately mobile robot motion in presence of sliding, a half turn tracking has been achieved with a 5 tons Claas tractor on a wet grass ground, at a 8 km/H speed. A classical path tracking control law constructed on rolling without sliding assumption (such as proposed in [18] or in [16]) has been used. The actual tracking error is reported in black solid line on figure 3. Firstly, we can notice that before and after the half turn (the curve is encountered between curvilinear abscissa 18 an 34m) the lateral deviation is satisfactorily around zero (straight line tracking on an even ground does not generate any sliding). On the contrary, during the half turn an almost constant deviation of 55cm is recorded, due to bad adherence properties neglected in the control law based on the classical Ackermann model (1).

The sliding parameters supplied by observation laws (8) and (9) (respectively BBKM and TBKM) allow to reflect this quite important deviation. The error reconstructed using BBKM is depicted on the same figure in green dotted line, while the red dashed line depicts the error reconstructed thanks to TBKM. It can be noticed that these signals are well

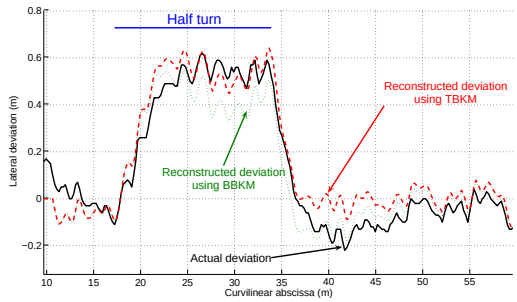

Fig. 3. Results of lateral deviation estimated vs actual deviation

superposed to the actual deviation, showing the capability of both of the extended models to reflect mobile robot motion in presence of sliding. Nevertheless, some small observation errors can be noticed on this figure, reflecting differences in the behavior of each models. A null reconstructed lateral deviation can be observed when relying on TBKM when leaving the curve (despite of the overshoot recorded on the actual deviation) when a steady error is present with BBKM.

III. Motion control with sliding accounted

A. Possible control approaches with extended models

The two extended kinematic models introduced in the previous section propose a relevant alternative to complete dynamic ones, since they can accurately describe actual mobile robot motion in presence of sliding with only a limited number of parameters. Moreover, since classical kinematic structure of mobile robot has been preserved, standard and efficient control approaches remain applicable: the large developments achieved in the field of mobile robotics such as described for instance in [2], [7] or [10], can benefit to these extended models, coupled with their dedicated observer. Depending on the considered model, the sliding parameters act differently. As a result, different control strategies appear to be more adapted to one or other point of view.

1) BBKM: In the Behavior Based Kinematic Model, the sliding parameters can be viewed as a disturbance acting on the ideal mobile robot motion that would have been obtained if rolling without sliding conditions were satisfied. As a consequence, it appears more suitable to apply control laws dedicated to perturbation rejection.

A first strategy can then consist in rejecting such perturbations by a robust approach without estimating accurately the sliding parameters: in this case, only the structure of the extended model is used. For instance, sliding mode control (as achieved in [6]) can be considered. Such approaches are efficient from a theoretical point of view, but inevitable actuator delays on steering wheel generate a chattering effect, which could be harmful in practice. Such a control law, applied only on front steering wheels (see [6] for details), has been tested on a loop path tracking on a paddy field, at a 6km/H speed. The experimental result is reported in red dashed line in figure 4 and compared to classical control law neglecting sliding effects, depicted in black solid line.

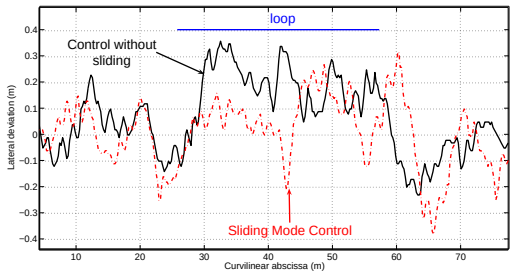

Fig. 4. Loop path tracking error using Sliding Mode Control law

A second strategy for perturbation rejection consists in taking part of the sliding parameters estimation capability. As demonstrated previously, the sliding parameters can indeed be on-line estimated by (8). Then, the contribution of sliding to the lateral deviation observed if the mobile robot is controlled under rolling without sliding assumption can be computed. As a consequence, this estimated deviation can be entered as an additive set point into the classical control law. In this strategy, the control structure is not modified, but an offset is entered, corresponding to the theoretical deviation calculated on-line from sliding estimation and model (4). This approach, detailed in [11], can be viewed as an Internal Model Adaptive control law. It has been tested in full scale experiments in the same conditions than those mentioned herebefore. The tracking deviation is reported in green dotted line in figure 5. It can be seen that after a transition phases appearing at the beginning of the curve (between curvilinear abscissas 30 and 42 m), the lateral deviation satisfactorily converges to zero. The sliding effects are compensated, without oscillations due to the chattering effect pointed out on figure 4, even if some overshoots can appear at curvature transitions.

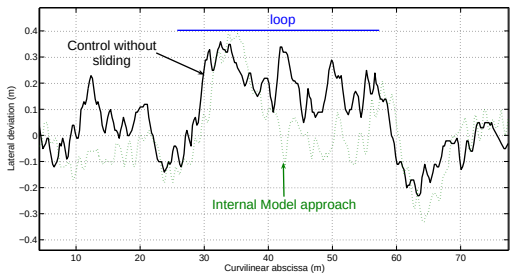

Fig. 5. Loop path tracking error using Internal Model Adaptive Control

2) TBKM: In this model point of view, sliding is entered as variables acting inside the model structure and respecting a kind of nonholonomic constraint to be accounted by control laws. The main interest is that the model structure stays unchanged with respect to the case where no sliding was accounted. A chained system transformation, equivalent to the one achieved in the rolling without sliding case, can

then be derived. An observer based adaptive control law, accounting for sliding effects, can then be designed. Such a control law has been proposed in [12], when only the front wheel is steered. Path tracking results obtained in the same conditions than those mentioned herebefore are presented in blue dashed dotted line in figure 6.

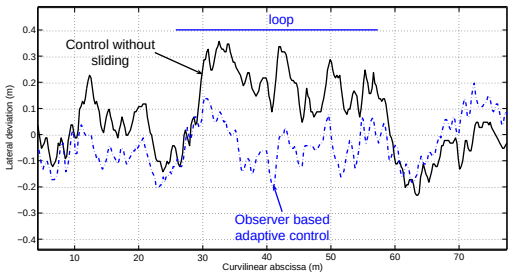

Fig. 6. Loop path tracking error using Observer Based Adaptive Control

It can be checked that this approach permits to compensate for sliding effects during the constant curvature phases (the lateral deviation reaches zero and stays null during the loop - from curvilinear abscissa 38m to 60m). It is also more reactive as overshoots recorded when entering or exiting the curve are limited. This particular point will be addressed in the section C.

B. Example of 4WS Backstepping Control

In order to illustrate the potentialities of extended kinematic models when addressing control design in presence of sliding, the extension of above-mentioned control laws to four wheeled-steering mobile robots is here discussed. With such robots, an attractive objective consists in controlling simultaneously the path tracking error y to zero and the angular deviation $\tilde{\theta}$ to a desired set point (hereafter denoted $\tilde{\theta}_{ref}$) with the two control inputs δ_F and δ_R. As the TBKM has been shown to be more accurate, this model is used below.

1) Front steering axle control: The expression of extended kinematic model (5), where sliding effects are accounted, is still consistent with classical models of wheeled mobile robots derived under non-sliding assumption. As a consequence, relying on [16], this model can be turned into an almost linear model, named chained form without any approximation. If δ_R is transiently considered as a parameter, then the first control input δ_F can easily be designed from this chained form in order to servo the lateral deviation. This constitutes the first step of the proposed backstepping approach. In a second step, the control input δ_R will be designed with the aim to servo the angular deviation.

Chained transformation of TBKM model (5) can be achieved relying on variables transformation (11)

$$\begin{array}{rcl} [s, y, \tilde{\theta}] & \rightarrow & [a_1, a_2, a_3] = [s, y, (1 - c\, y)\tan(\tilde{\theta} + \beta_{R2})] \\ [v, \delta_F] & \rightarrow & [m_1, m_2] = [\frac{V_r \cos(\tilde{\theta}+\beta_{R2})}{1-c(s)\, y}, \frac{da_3}{dt}] \end{array} \quad (11)$$

and leads to the following chained system:

$$\left\{ \begin{array}{rcl} \dot{a}_1 = \frac{d\, a_1}{dt} & = & m_1 \\ \dot{a}_2 = \frac{d\, a_2}{dt} & = & a_3 m_1 \\ \dot{a}_3 = \frac{d\, a_3}{dt} & = & m_2 \end{array} \right. \quad (12)$$

When introducing derivatives with respect to the curvilinear abscissa, model (12) can be expressed as:

$$\left\{ \begin{array}{rcccl} a_2' & = & \frac{da_2}{da_1} & = & a_3 \\ a_3' & = & \frac{da_3}{da_1} & = & m_3 = \frac{m_2}{m_1} \end{array} \right. \quad (13)$$

The lateral deviation can then be controlled by designing m3 according to (14), since it leads to a second order differential equation, ensuring the convergence of $a_2 = y$ to zero.

$$m_3 = -K_d a_3 - K_p a_2 \quad (K_d, K_p > 0) \quad (14)$$

Injecting (14) into (11), and considering $\delta_R - \beta_R$ as slow-varying with respect to the dynamic imposed by the two gains K_p and K_d, leads to the following expression for the first control input δ_F:

$$\begin{array}{rcl} \delta_F & = & \arctan\Big\{ \tan(\delta_R - \beta_R) \\ & & + \frac{L}{\cos(\delta_R - \beta_R)} \big(\frac{c(s)\cos\tilde{\theta}_2}{\alpha} + \frac{A \cos^3\tilde{\theta}_2}{\alpha^2} \big) \Big\} + \beta_F \end{array} \quad (15)$$

with:

$$\left\{ \begin{array}{rcl} \tilde{\theta}_2 & = & \tilde{\theta} + \delta_R - \beta_R \\ \alpha & = & 1 - c(s) y \\ A & = & -K_p y - K_d\, \alpha \tan\tilde{\theta}_2 + c(s) \alpha \tan^2\tilde{\theta}_2 \end{array} \right. \quad (16)$$

Since derivatives with respect to the curvilinear abscissa is here considered, the gains (K_p, K_d) allow to specify a settling distance instead of a settling time. In the sequel, it is chosen $K_p = \frac{K_d^2}{4}$ in order to obtain a critical damping $\xi = 1$. Finally, it can be noticed that the classical control law designed under rolling without sliding assumption (such as derived in [18]) can be recovered when setting sliding parameters β_F and β_R to zero:

$$\begin{array}{rcl} \delta_F & = & \arctan\Big\{ L \big(\frac{c(s)\cos\tilde{\theta}}{\alpha} + \frac{\cos^3\tilde{\theta}}{\alpha^2} [K_p y \\ & & - K_d\, \alpha \tan\tilde{\theta} + c(s) \alpha \tan^2\tilde{\theta}] \big) \Big\} \end{array} \quad (17)$$

2) Backstepping control for rear axle: With control law (15), the lateral deviation is satisfactorily servoed to zero, as well as $\tilde{\theta}_2$. The convergence of this latter variable implies that actual angular deviation $\tilde{\theta}$ converges to $\beta_R - \delta_R$, and not to some desired set point, as expected. Actual control of $\tilde{\theta}$ can now be addressed using the control input δ_R. This constitutes the second step of the proposed control approach.

Reporting control law (15) into the third equation in model (5) leads to the following angular deviation dynamic with respect to curvilinear abscissa:

$$\tilde{\theta}' = \big(-\frac{K_d^2\, y}{4\, \alpha} - K_d \tan\tilde{\theta}_2 + c(s) \tan^2\tilde{\theta}_2 \big) \cos^2\tilde{\theta}_2 \quad (18)$$

As above mentioned, control law (15) imposes that $\tilde{\theta}_2$ stays close to zero. As a result, the term $\cos^2\tilde{\theta}_2$ can be considered as equal to 1, so that:

$$\tilde{\theta}' = -\frac{K_d^2\, y}{4\,\alpha} - K_d \tan\tilde{\theta}_2 + c(s)\tan^2\tilde{\theta}_2 \qquad (19)$$

In view of (19), two cases must be distinguished, according to the curvature value:

If the case $c(s)$=0 (straight line following) is encountered, the angular deviation dynamic (19) can be simplified as:

$$\tilde{\theta}' = -\frac{K_d^2\, y}{4} - K_d \tan\tilde{\theta}_2 \qquad (20)$$

Then, the error dynamic $\tilde{\theta}' = K_{d2}\,(\tilde{\theta}_{ref} - \tilde{\theta})$ with $K_{d2} > 0$ can easily be imposed by proposing the following rear steering law:

$$\delta_R = \beta_R - \tilde{\theta} + \arctan\Big(\frac{-K_d\, y}{4} - \frac{K_{d2}\,(\tilde{\theta}_{ref} - \tilde{\theta})}{K_d}\Big) \qquad (21)$$

This ensures the convergence of $\tilde{\theta}$ to $\tilde{\theta}_{ref}$.

Now **in the case $c(s) \neq$0 (curved path following)**, using the notation $W = \tan\tilde{\theta}_2$, equation (19) can be rewritten as:

$$-\tilde{\theta}' - \frac{K_d^2\, y}{4\,\alpha} - K_d\, W + c(s)\, W^2 = 0 \qquad (22)$$

Once more, the objective is to impose $\tilde{\theta}' = K_{d2}\,(\tilde{\theta}_{ref} - \tilde{\theta})$. If it was achieved, then the discriminant of equation (22) would be (using $\alpha = 1 - c(s)y$):

$$\Delta = \frac{K_d^2}{\alpha} - 4\, c(s)\, K_{d2}\,(\tilde{\theta} - \tilde{\theta}_{ref}) \qquad (23)$$

As α is assumed to be always strictly positive, see hypothesis (3), the condition $\Delta > 0$ leads to:

$$\begin{cases} (\tilde{\theta} - \tilde{\theta}_{ref}) & < & \frac{K_d^2}{4\, c(s)\, K_{d2}\, \alpha} & if\ c(s) > 0 \\ (\tilde{\theta} - \tilde{\theta}_{ref}) & > & \frac{K_d^2}{4\, c(s)\, K_{d2}\, \alpha} & if\ c(s) < 0 \end{cases} \qquad (24)$$

The choice for (K_d, K_{d2}) and the limit values of $c(s)$ and y lead, in the worse case, to a $\pm 30°$ bound on $(\tilde{\theta} - \tilde{\theta}_{ref})$, which is always satisfied in practice when properly initialized.

Since Δ has been shown to be strictly positive, two solutions for W can be derived. Considering the range of variation of the actutors, only one of the solutions can be applied. As a result, the rear control law achieving the expected convergence can be written as following:

$$\delta_R = \beta_R - \tilde{\theta} + \arctan\left\{\frac{K_d - \sqrt{\frac{K_d^2}{\alpha} - 4\, c\, K_{d2}\,(\tilde{\theta} - \tilde{\theta}_{cons})}}{2c(s)}\right\} \qquad (25)$$

Expressions (21) and (25) constitute the rear steering law for respectively straight and curve line following. The continuity of these expressions, when $c(s)$ tends to zero, can be established by standard but tedious computations.

3) Stability of the backstepping controller: The stability of the overall non-linear control strategy, composed of control law (15) for the front steering angle and (21)-(25) (depending on $c(s)$ value), can be checked using Lyapunov theory.

Consider Lyapunov function candidate:

$$V = \tfrac{1}{2}\Big\{y^2 + (\alpha\tan\tilde{\theta}_2)^2 + \epsilon^2\Big\} \qquad (26)$$

with $\epsilon = \tilde{\theta}_{ref} - \tilde{\theta}$.

The derivative of the positive function V with respect to curvilinear abscissa (homogeneous with the time derivative since robot velocity is assumed to be non-null) leads, after calculations, to the following expression (whatever the curvature value):

$$\frac{dV}{ds} = -K_d\alpha^2\tan^2\tilde{\theta}_2 - K_{d2}(\epsilon\cos\tilde{\theta}_2)^2 \qquad (27)$$

which is always negative. The stability of the mobile robot trajectory tracking and the convergence of both ϵ and $\tilde{\theta}_2$ to zero is then ensured. Then, injecting the null asymptotic value of $\tilde{\theta}_2$ into equation (18) establishes that the lateral deviation y also converges to zero. This finally demonstrates the stability of path tracking control in presence of sliding, with respect to lateral and angular deviations, with front and rear control laws (15) and (21) if $c(s) = 0$ or (15) and (25) if $c(s) \neq 0$.

Such a control algorithm permits to compensate for sliding effects: experimental tests corroborat that lateral deviation converges to zero while angular deviation converges to the desired set point. Nevertheless, if theoretical simulations neglecting actuator behavior supply high accurate results, some overshoots can unfortunately be recorded at transition phases, and more particularly at path curvature transitions during full-scale experiments. These overshoots, are mainly due to low level delays and inertial effects (it can be checked on theoretical simulations by introducing delays on steering angle response): the mobile robot indeed starts to turn one moment after the steering variables have been sent to the actuators.

C. Predictive curvature servoing

In order to compensate for actuator delay and then cancel overshoots at curvature transitions, a partial model predictive control can be coupled with the previous approach. In this paper, such a prediction is applied only on front wheels (δ_F), since rear axle is mainly used to control angular deviations, on which low level delays are less penalizing. The objective is to send steering control signal before entering a curve (according to actuator delay) in order to obtain a relevant actual steering angle as soon as the curve appears. Following the same methodology than the one detailed in [12], it is considered that a low level model is available, and that the future path curvature can be known in advance. As the adherence conditions cannot be predicted, the control law (15) used for the front steering wheel can be split into two additive terms. Using the trigonometrical function:

$$\arctan(a+b) = \arctan(a) + \arctan(\tfrac{b}{1+ab+b^2}) \qquad (28)$$

the control law (15) can be divided as follows:

$$\delta_F = \delta_F^{Traj} + \delta_F^{Dev}$$
$$\begin{cases} \delta_F^{Traj} &= \arctan(a) \\ \delta_F^{Dev} &= \arctan(\frac{b}{1+ab+b^2}) + \beta_F \end{cases} \quad (29)$$

where:
$$a = \frac{L}{\cos(\delta_R - \beta_R)} c(s) \frac{\cos\tilde{\theta}_2}{\alpha}$$
$$b = \frac{L}{\cos(\delta_R - \beta_R)} A \frac{\cos^3\tilde{\theta}_2}{\alpha^2} + \tan(\delta_R - \beta_R)$$

In this decomposition, δ_F^{Dev} is mainly concerned with deviation and is equal to zero when both sliding and deviations are null, while δ_F^{Traj} ensures the convergence of mobile robot curvature to the trajectory one (non null term when both sliding and deviations are null). As a consequence, the predictive algorithm will be applied only on this latter term in order to anticipate the variations of the path curvature to be followed. The proposed prediction algorithm follows the scheme depicted in figure 7.

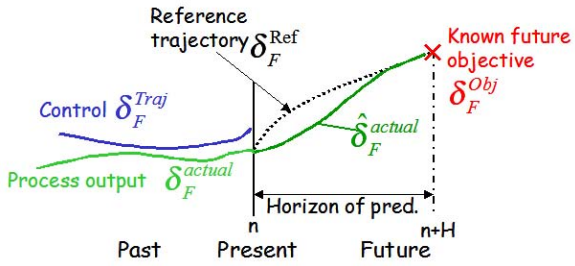

Fig. 7. Prediction principle

At each time t, the future trajectory is considered along a fixed horizon of prediction called H. The corresponding curvature at time $t+H$ is extracted and allows to compute an objective δ_F^{Obj} to be reached by the front wheel angle if deviation and sliding could be neglected (these two elements are addressed by the term δ_F^{Dev}). Knowing the value of angle δ_F^{Traj} at current time and the objective to be reached at time $t+H$, a reference shape, called δ_F^{ref}, ensuring this convergence can be chosen on the horizon of prediction (typically the output of a first order transfer function). From the actuator model, the evolution of term δ_F^{Traj} to a given sequence of control send to actuator can then be predicted: it is called $\hat{\delta}_F^{actual}$. Finally, the prediction algorithm consists in finding the sequence of control, minimizing the difference $\hat{\delta}_F^{actual} - \delta_F^{Ref}$ on the horizon of prediction H. The predictive angle to be applied for curvature anticipation is then the first value of the minimizing sequence, called δ_{Pred}^{Traj}.

This predictive term δ_{Pred}^{Traj} is then substituted to the trajectory term δ_F^{Traj}, as described in figure 8. The front steering angle sent to the actuator is then:

$$\delta_F = \delta_F^{Dev} + \delta_{Pred}^{Traj} \quad (30)$$

while rear steering control law stays unchanged.

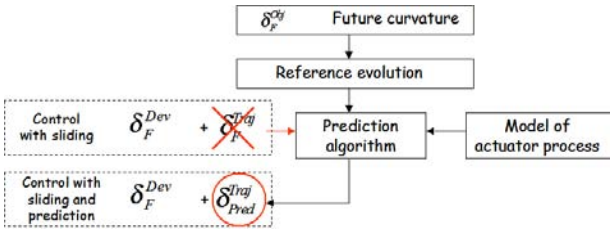

Fig. 8. General algorithm of curvature prediction

IV. Experimental results

A. Experimental mobile robots

In order to demonstrate the capability of control laws (30) and (21)-(25) for accurately guiding four-steered wheeled mobile robots on natural ground, the experimental electric platform depicted in figure 9 has been used. The vehicle weight and maximum speed are respectively 600 kg and 18 km/h, and it can climb slopes up to 45°. The only on-boarded exteroceptive sensor is an RTK-GPS receiver, whose antenna has been located straight up the middle of the rear axle. It supplies an absolute position accurate to within 2cm, at a 10Hz sampling frequency. A Kalman filter is used to estimate the mobile robot heading.

Fig. 9. Experimental platform

Sliding compensation in path tracking application has been investigated via two experiments, where sliding is very likely to occur: a straight line following on a sloping ground and a curved line following on an even ground.

B. Straight line following on a slope

In this configuration, a straight line reference path has been computed perpendicularly to a slope on a grass soil, as shown in figure 9. Two path tracking were achieved successively at a 2m/s speed. The first one was achieved relying on the standard control law neglecting sliding for front steering (17) and without any rear steering ($\delta_R = 0$). The tracking error and angular deviation are reported respectively in figures 10(a) and 10(b) in black solid line. The second path tracking was completed relying on the proposed front and rear control laws (30) and (21)-(25) when specifying a null desired angular deviation ($\tilde{\theta}_{ref} = 0$). The results of this second test are reported in figures 10(a) and 10(b) in green dotted line.

First of all, the effect of sliding on a classical approach can be observed: figure 10 shows that the tracking error as well as the angular deviation cannot reach the desired zero value

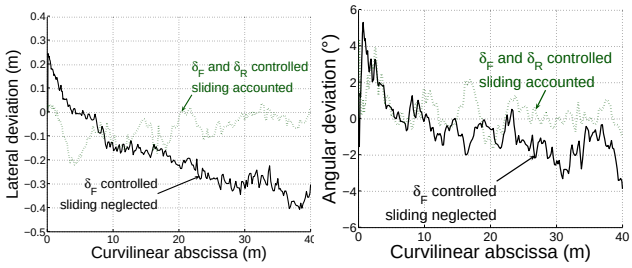

(a) Lateral deviation (b) Angular deviation

Fig. 10. Path tracking in slope with $\tilde{\theta}_{ref} = 0$

(the lateral deviation converges close to -30cm while the angular deviation reaches -2°). On the contrary, when relying on the proposed algorithm exploiting the two steering axles, the mobile robot is able to reach null lateral and angular deviations, despite the sliding effects. The robot can then compensate sliding and follows accurately the trajectory with respect to both the lateral and the angular errors.

Moreover, rear steering control allows to reach any desired relative orientation. This fact is illustrated in figure 11, where the same path has been tracked when specifying different set points for angular deviation:

- $\tilde{\theta}_{ref} = 0°$ depicted in black solid line
- $\tilde{\theta}_{ref} = -10°$ depicted in red dashed line
- $\tilde{\theta}_{ref} = -20°$ depicted in green dotted line

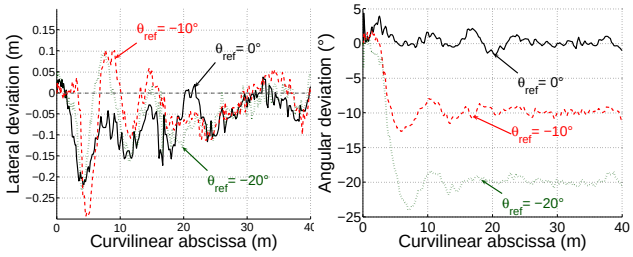

(a) Lateral deviation (b) Angular deviation

Fig. 11. Path tracking in slope with different $\tilde{\theta}_{ref}$

It can be checked that the accuracy of path tracking is preserved whatever the choice for $\tilde{\theta}_{ref}$ (i.e. lateral deviation converges to zero whatever $\tilde{\theta}_{ref}$), while $\tilde{\theta}$ satisfactorily reaches its set point. This demonstrates the capability of the proposed algorithm to control independently lateral and angular deviations, despite sliding phenomena.

C. curved path following

In this configuration, the reference path is a half turn recorded on an even slippery ground. As previously, two path tracking were achieved: one relying on the classical control law (17), and the other one relying on the proposed approach. A desired angular deviation of -10° has been specified in order to highlight rear steering actuation potentiality. Path tracking are shown in figure 12: the black solid line depicts the lateral deviation recorded when sliding is neglected and when only the front axle is controlled, while the red dashed line reflects the tracking error obtained when relying on control laws (30) and (21)-(25).

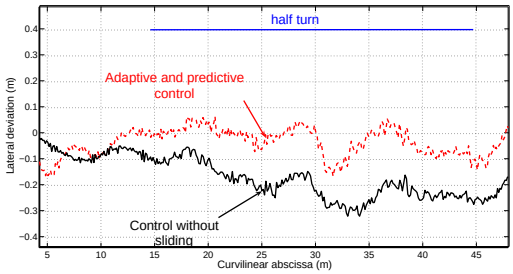

Fig. 12. Path tracking errors during curve path following

As expected, the proposed algorithm ensures that the mobile robot reaches a null lateral deviation. In contrast, when relying on classical control law, a 25cm steady lateral deviation is noticed. Moreover, it can be observed that the path tracking accuracy is not affected by curvature transitions occuring at the beginning and at the end of the curve (at curvilinear abscissa 15m and 45m), demonstrating the relevancy of the proposed predictive curvature servoing. The lateral deviation stays satisfactorily close to zero all path long. To go further, figure 13 shows the relative angular orientation. As desired, it converges accurately to the desired

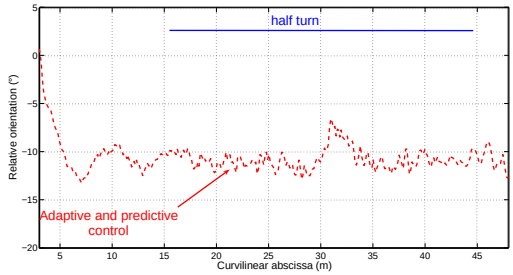

Fig. 13. Relative orientations during curve path following

set point $\tilde{\theta}_{ref}$=-10° and maintains this value during all the path tracking. On both figures, a short deviation can be observed at curvilinear abscissa 32m, corresponding to a hole crossing on one side of the robot.

V. Conclusions and Future Work

This paper proposes a high accurate control strategy dedicated to path tracking for mobile robots in off-road environment. It indeed allows to take into account for disturbing phenomena, without requiring the use of complex dynamic models, which classically need numerous parameters hardly observable in off-road conditions. The proposed approach is based on extended kinematic models designed for a generic two wheeled steered vehicle. Sliding phenomena is accounted via a limited number of variables, on-line observable with classical embedded perception systems. The influence

of bad adherence properties on the robot motion can then be described, while preserving the kinematic structure of the model, so that traditional control techniques can still be used. A control approach, relying on such models, is thus designed, and the efficiency of sliding effects compensation has been investigated through experimental results. More precisely, a control law based on chained systems is detailed. It ensures the convergence of the mobile robot to its reference path, with a vehicle relative orientation converging to a desired set point. In addition, a predictive curvature servoing is designed to tackle the effect of delays induced by both actuators and robot inertia. This predictive action allows to preserve tracking accuracy from overshoots at path curvature transitions (entering/exiting a curve). When the adaptive approach (with on-line sliding estimation) and prediction are coupled, the mobile robot is able to follow accurately (up to a few centimeters - i.e. sensor precision) a trajectory whatever the shape to be followed and the adherence conditions.

Current developments on the proposed algorithm are focused on two points. First, the curvature predictive control does not take explicitly vehicle inertia into account: only the actuator model is used. The tuning parameters of the model predictive algorithm allow to compensate indirectly the inertia. Nevertheless, a partial dynamic model including for inertial effect is expected to be introduced. The second point deals with sliding parameters on-line observation. Currently, no model for sliding parameters evolution is considered in observer algorithm, so that limited overshoots can be observed when conditions quickly change. The use of a partial contact model in the designed observer, able to describe some sliding dynamics, could permit to improve estimation reactivity and finally the control loop performances. In counterpart, this could imply the use of additional sensors, such as gyrometer or IMU (in order to measure state derivatives).

More generally, the overall control algorithm proposed in this paper has been actually validated at speeds up to 3 m/s. Current developments aim at increasing the mobile robot speed in order to extend autonomy on unstructured ground (10 m/s is the objective). This requires the use of higher sampling frequencies (equal to 10Hz, i.e. the GPS rate). This can also require the use of additional sensors. Moreover, at such speed 3D effects (such as roll), neglected in this paper, may have to be accounted in order to ensure mobile robot stability.

REFERENCES

[1] C. Canudas de Wit, H. Olsson, K.J. Astrom, and P. Lischinsky, *A new model for control of systems with friction*, IEEE Transactions on Automatic Control **40** (1995), no. 3, 419–425.

[2] C. Canudas de Wit, B. Siciliano, and G. Bastin, *Theory of robot control.*, The Zodiac, 1996.

[3] L.M. Corradini, T. Leo, and G. Orlando, *Experimental testing of a discrete-time sliding mode controller for trajectory tracking of a wheeled mobile robot in the presence of skidding effects*, Journal of Robotic System **19** (2002), no. 4, 177–188.

[4] C. Grand, F. Ben Amar, F. Plumet, and P. Bidaud, *Stability and traction optimization of a reconfigurable wheel-legged robot*, International Journal of Robotics Research **23** (2004), no. 10-11, 1041–1058.

[5] H.F. Grip, L. Imsland, T.I. Fossen, J.C. Kalkkuhl, and A. Suissa, *Nonlinear vehicle velocity observer with road-tire friction adaptation*, Proceedings of the IEEE Conference on Decision and Control, 2006, pp. 3603–3608.

[6] F. Hao, R. Lenain, B. Thuilot, and P. Martinet, *Robust adaptive control of automatic guidance of farm vehicles in the presence of sliding*, IEEE International Conference on Robotics and Automation (Barcelona (Spain)), 2005, pp. 3113–3118.

[7] J. Hermosillo and S. Sekhavat, *Feedback control of a bi-steerable car using flatness application to trajectory tracking*, American Control Conference, vol. 4, 2003, p. 3567:3572.

[8] F. Holzmann, M. Bellino, R. Siegwart, and H. Bubb, *Predictive estimation of the road-tire friction coefficient*, Proceedings of the IEEE International Conference on Control Applications, 2007, pp. 885–890.

[9] G. Ishigami, K. Nagatani, and K. Yoshida, *Path following control with slip compensation on loose soil for exploration rover*, IEEE International Conference on Intelligent Robots and Systems, 2006, pp. 5552–5557.

[10] J-P. Laumond, *La robotique mobile*, Systmes automatisés (IC2), Hermes, Paris, 2001.

[11] R. Lenain, B. Thuilot, C. Cariou, and P. Martinet, *Adaptive control for car like vehicles guidance relying on rtk gps: Rejection of sliding effects in agricultural applications*, Proceedings - IEEE International Conference on Robotics and Automation (Tapei (Tawan)), vol. 1, 2003, pp. 115–120.

[12] ———, *High accuracy path tracking for vehicle in presence of sliding: Application to farm vehicles automatic guidance for agricultural task*, Autonomous Robots **21** (2006), no. 1, 79–97.

[13] ———, *Adaptive and predictive path tracking control for off-road mobile robots*, European Journal of Control **13** (2007), no. 4, 419–439.

[14] L. Ojeda and J. Borenstein, *Methods for the reduction of odometry errors in over-constrained mobile robots*, Autonomous Robots **16** (2004), no. 3, 273–286.

[15] H.B. Pacejka, *Tire and vehicle dynamics*, Society of Automotive Engineers, 2002.

[16] C. Samson, *Control of chained system*, IEEE Transactions on Automatic Control **40** (1995), no. 1, 64–77.

[17] L. Seddiki, A. Rabhi, N.K. M'Sirdi, and Y. Delanne, *Analyse comparative des modèles de pneumatiques contact roue-sol*, IEEE Conférence Internationale Francophone d'Automatique (Bordeaux, France), 2006.

[18] B. Thuilot, C. Cariou, P. Martinet, and M. Berducat, *Automatic guidance of a farm vehicle relying on a single cp-gps*, Autonomous Robots **13** (2002), no. 2, 53–71.

[19] D. Wang and C.B. Low, *An analysis of wheeled mobile robots in the presence of skidding and slipping: Control design perspective*, IEEE International Conference on Robotics and Automation (Roma, Italy), 2007, pp. 2379–2384.

[20] Y. Zhang, J.H. Chung, and S.A. Velinsky, *Variable structure control of a differentially steered wheeled mobile robot*, Journal of Intelligent and Robotic Systems: Theory and Applications **36** (2003), no. 3, 301–314.